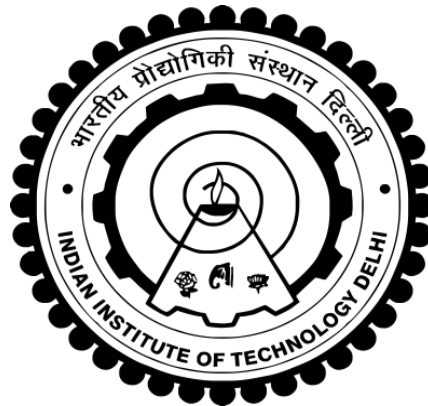


# **CONTROL OF GRID INTEGRATED MULTIPLE SOLAR PV ARRAYS-BATTERY BASED MICROGRID SYSTEM**

**SHUBHRA**



**DEPARTMENT OF ELECTRICAL ENGINEERING**

**INDIAN INSTITUTE OF TECHNOLOGY DELHI**

**AUGUST 2021**

© **Indian Institute of Technology Delhi (IITD), New Delhi, 2021**

# **CONTROL OF GRID INTEGRATED MULTIPLE SOLAR PV ARRAYS-BATTERY BASED MICROGRID SYSTEM**

*by*

**SHUBHRA**

**Department of Electrical Engineering**

*Submitted*

**in fulfilment of the requirements of the degree of Doctor of philosophy**

**to the**



**INDIAN INSTITUTE OF TECHNOLOGY DELHI**

**AUGUST 2021**

# **CERTIFICATE**

It is certified that the thesis entitled “**Control of Grid Integrated Multiple Solar PV Arrays-Battery Based Microgrid System,**” being submitted by **Mrs. Shubhra** for award of the degree of **Doctor of Philosophy** in the Department of Electrical Engineering, Indian Institute of Technology Delhi, is a record of the student work carried out by her under my supervision and guidance. The matter embodied in this thesis has not been submitted for award of any other degree or diploma.

**Dated:**

**(Prof. Bhim Singh)**  
**Electrical Engineering Department**  
**Indian Institute of Technology Delhi**  
**Hauz Khas, New Delhi-110016, India**

## ACKNOWLEDGEMENTS

I wish to express my sincere gratitude and indebtedness to **Prof. Bhim Singh** from bottom of my heart for valuable guidance and constant supervision to carry out the Ph.D. work. It was an unique and rewarding learning experience to work under him throughout the research period, which has provided me with a deep insight to the world of technical quality research. The commitment, discipline, determination, dedication, resourcefulness and above all innovative approach of **Prof. Bhim Singh** have been the main inspiration for me to complete this work. His valuable advice, consistent guidance, continuous monitoring and daily encouragement and commitments to achieve excellence have motivated me to improve my work and make best use of my capabilities. It was due to his blessing that I have experienced numerous new traits of technical research that will help me throughout my life.

I express my deep gratitude and sincere thanks to **Prof. Sukumar Mishra, Prof. G. Bhuvaneswari and Prof. Ashu Verma**, SRC members for their valuable guidance and consistent support throughout my research work.

I wish to convey my sincere thanks to **Prof. Bhim Singh, Prof. B. P. Singh, Prof M.L. Kothari and Prof. Anandarup Das** for their valuable inputs during my course work, which made the strong foundation for my research work. I am grateful to IIT Delhi as an institute for providing me the requisite research facilities. Thanks are due to Sh. Srichand, Sh. Puran Singh and Mr. Jitendra of PG Machine lab for providing me facilities and assistance during this work. I am thankful to Dr. Chinmay Jain, Dr. Geeta Pathak, Dr. Shailendra Kumar, Dr. Ikhlq Hussain, Dr. Rajan Sonkar, Dr. Aniket Anand, Dr. Sachin Devassy, Dr. Nidhi Mishra, Dr. Nishant Kumar, Dr. Sai Pranith Girimaji, Dr. Anjanee Mishra, Dr. Piyush Kant, Dr. Saurabh Shukla, Dr. Shadab Murshid, Dr.

Deepu Vijay, Dr. Priyank Shah, Dr. V.L. Srinivas and Mr. Anshul Varshney for their valuable aid and co-operation and informal support during this period.

I convey my sincere thanks to Ms. Farheen Chisti and Ms. Pavitra Shukl for motivation, co-operation and informal support during my research work. I would like to thank Ms. Rohini Sharma, Mr. P. Sambasivaiah and Mr. Munesh Kumar Singh for being supportive. I am thankful to Mr. Vineet P. Chandran, Dr. Tipurari Nath Gupta, Dr. Radha Kushwaha, Ms. Shatakshi Sharma, Ms. Seema and Ms. Vanadana Jain, for their valuable aid and co-operation.

Moreover, I would like to thank, Mr. Sreejith R, Mr. Gurmeet Singh, Mr. Anjeet Verma, Mr. Debasish Mishra, Ms. Subarni Pradhan, Dr. Tabish Mir, Mr. Utkarsh Sharma, Mr. K. P. Tomar, Mr. Sunil Kumar Pandey, Ms. Yashi Singh, Ms. Hina Parveen, Ms. Rashmi Rai, Mr. Yalavarthi Amarnath, Mr. Arayadip Sen, Mr. Kashif, Mr. Gaurav Modi, Mr. Sudip Bhattacharya, Mr. Bilal Naqvi, Mr. Jitendra Gupta, Mr. Utsav Sharma, Mr. Sandeep Kumar Sahoo, Ms. Shalvi Tyagi, Mr. Souvik Das, Mr. Vivek Narayanan, Saran Chaurashiya, Mr. Sharan Shastri, Mr. Shivam Yadav, Mr. Rahul Kumar, Mr. Deepak Saw, Ms. Kousalya V, Ms. Chandrakala Devi, Ms. Kripa and all PG Machines lab group for their valuable support.

I would also like to thank Mr. Yatindra Tripathi, Mr. Satish, Mrs. Sunita Verma, Ms. Moni, Mr. Sandeep and all other Electrical Engineering office staff for being supportive throughout my work. I thank all those who have directly or indirectly helped me to complete my dissertation.

The completion of this work was not possible without the blessings of my mother, Late Mrs. Arun Prabha. I would like to thank my father, Prof. Vir Singh for his consistent blessings and encouragement during the entire journey of my research work. I would like to thank my husband Mr. Bhupender Singh, my daughter Shaurya and my son Siddhnat for giving me the all requisite support during my research work. Their trust in my capabilities had been a key factor to all my

achievements. I would like to thank my sisters Abha and Puja, brother Vijay and their families for their continuous support and encouragement. I would like to thank my in-laws for their support and blessings.

I am indebted to almighty for their blessings to elevate my academic level and granting me the wisdom, health and strength to undertake this research task and enabling me to its completion.

Dated:

Shubhra

## ABSTRACT

The microgrid comprises of distributed energy resources, battery energy storage (BES) and loads. Microgrid operates in standalone as well as grid connected modes. The integration of microgrid to the utility grid enhances the reliability and efficiency of system. The continuously increasing demand of electrical power, fossil fuels diminution and environmental concerns have resulted in the progression of renewable energy sources (RESs) i.e. hydro, wind and solar etc. Among the RESs, the solar power generation is clean and inexpensive. In grid integrated solar PV system, one PV array is used, however, due to the intermittent nature of solar PV power and loads, the off-grid mode operation is not reliable. At the grid outage/fault and non-accessibility of the solar PV array power, uninterrupted power is not delivered to the loads. Therefore, BES plays an important role at grid outage and unavailability of solar PV power and supplies power to the critical loads.

This work aims at the design, control and operation for various configurations of three-phase three-wire and three-phase four-wire single solar PV array-BES with a bidirectional converter systems and multiple solar PV arrays-BES based microgrids with synchronization to the grid. In these configurations above stated issues are addressed and continual power during the grid outage to the load side is ensured. A single voltage source converter (VSC) is utilized for DC to AC power conversion in three phase grid connected solar PV- BES with a bidirectional converter systems in a single stage topology. VSC operates with a current control and voltage control corresponding to the grid interactive and off-grid modes.

In three phase grid integrated multiple solar PV arrays-BES based microgrids, the DC links of main and ancillary VSCs are integrated with individual solar PV arrays through an individual maximum power point tracking (MPPT) technique. VSCs terminals are connected in parallel at the point of common coupling (PCC), which increases the power rating of microgrid and facilitates the microgrid expansion to distribute active power to the utility grid. It also improves the reliability of microgrid in an autonomous mode of operation. Under normal operating condition, the current control is used in the grid interactive mode for the main VSC, whereas at the grid disturbances, it operates with the voltage control to maintain the frequency and voltage at the PCC. A quality voltage is provided to the ancillary VSC, hence the current control is used for its operation. In the grid interactive mode, the grid maintains the voltage and frequency at the microgrid. Therefore, both VSCs operate with the current control algorithms.

In order to enhance the power rating of microgrid, resolving grid outage scenario and solve power

quality (PQ) concerns of the distribution network, numerous configurations of three phase multiple solar PV arrays-BES based microgrids are classified on the basis of battery connection at the DC link of the main VSC i.e. directly or through bidirectional converter, power conversion stages like, single stage or double stage and three phase supply i.e. three-phase three-wire or three-phase four-wire systems. In the three-phase grid integrated multiple solar PV arrays-BES based microgrids, a PV array is integrated in a double stage configuration at main VSC DC link, in which a DC-DC boost converter is utilized to obtain MPPT voltage in the first stage. Further, in the second stage, the main VSC is connected to the utility grid. The BES is also integrated directly at main VSC DC link and manages the load levelling. However, the second PV array is connected in a single stage configuration. In three phase grid integrated multiple solar PV arrays-BES with a bidirectional converter based microgrids, PV arrays are directly connected to the DC links of VSCs in a single stage configuration. The BES is integrated via a bidirectional converter at the main VSC DC link, which maintains its DC link voltage to the MPPT value and regulates the charging / discharging current of BES. In three phase grid integrated multiple solar PV arrays-based microgrids, two PV arrays of different power ratings, are connected to DC links of VSCs in a single stage topology and the main VSC provides active power is to the grid. In both the modes, VSCs regulate the load demands at their respective terminals. The PV power feed-forward component is utilized for the enhancement of system's dynamics and to distribute active power to the grid. The current control technique utilized in these configurations, improves the PQ issues such as harmonics current extenuation and power factor correction at the grid or at the grid forming converter. At no solar PV array power availability, VSC mode changes into the distribution static compensator (DSTATCOM) mode and the grid supplies the power to the loads. The three-phase four-wire multiple PV arrays-BES microgrids are utilized for mitigation of neutral current and to perform all other functions of three-phase three-wire system. These configurations are capable of distributing power to rooftop residential, industrial and commercial buildings, electric traction, electric vehicles, rural/remote areas and water pumping. The simulated performances of three-phase grid integrated single solar PV array-BES systems with a bidirectional converter and multiple solar PV arrays-BES based microgrids in the MATLAB/Simulink platform for various steady state and dynamic conditions are validated with experimental results on a developed prototype in the laboratory and through a real time controller OPAL-RT (OP4510) hardware in loop -test bench in RT-LAB platform, correspondingly.

## सारांश

माइक्रोग्रिड में वितरित ऊर्जा संसाधन, बैटरी ऊर्जा भंडारण (बीईएस) और लोड शामिल हैं। माइक्रोग्रिड स्टैंडअलोन के साथ-साथ ग्रिड कनेक्टेड मोड में काम करता है। यूटिलिटी ग्रिड में माइक्रोग्रिड का एकीकरण प्रणाली की विश्वसनीयता और दक्षता को बढ़ाता है। विद्युत शक्ति की लगातार बढ़ती मांग, जीवाश्म ईंधन की कमी और पर्यावरण संबंधी मुद्दों के परिणामस्वरूप अक्षय ऊर्जा स्रोतों (आरईएस) यानी हाइड्रो, विंड और सोलर आदि की प्रगति हुई है। आरईएस के बीच, सौर ऊर्जा उत्पादन स्वच्छ और सस्ती है। ग्रिड एकीकृत सौर पीवी प्रणाली में, एक पीवी सरणी का उपयोग किया जाता है, हालांकि, सौर पीवी पावर और लोड की आंतरायिक प्रकृति के कारण, ऑफ-ग्रिड मोड संचालन विश्वसनीय नहीं है। ग्रिड आउटेज/फॉल्ट और सोलर पीवी सरणी पावर की अगम्यता पर, लोड को निर्बाध बिजली नहीं दी जाती है। इसलिए, बीईएस ग्रिड आउटेज और सौर पीवी बिजली की अनुपलब्धता में एक महत्वपूर्ण भूमिका निभाता है और महत्वपूर्ण लोड को बिजली की आपूर्ति करता है।

इस कार्य का उद्देश्य तीन-चरण तीन-तार और तीन-चरण चार-तार विभिन्न विन्यासों के लिए एकल सौर पीवी सरणी-बीईएस के साथ एक द्विदिश कनवर्टर सिस्टम और एकाधिक सौर पीवी सरणियाँ-बीईएस आधारित माइक्रोग्रिड का ग्रिड के साथ सिंक्रनाइज़ेशन के साथ डिजाइन, नियंत्रण और संचालन करना है। इन विन्यासों में ऊपर बताए गए मुद्दों को संबोधित किया जाता है और ग्रिड आउटेज के दौरान लोड साइड को निरंतर बिजली सुनिश्चित की जाती है। एक एकल वोल्टेज स्रोत कनवर्टर (वीएससी) का उपयोग डीसी से एसी बिजली रूपांतरण के लिए तीन चरण ग्रिड से जुड़े सौर पीवी-बीईएस में एकल चरण टोपोलॉजी में एक द्विदिश कनवर्टर सिस्टम के साथ किया जाता है। वीएससी ग्रिड इंटरएक्टिव और ऑफ-ग्रिड मोड के अनुरूप करंट कंट्रोल और वोल्टेज कंट्रोल के साथ काम करता है।

तीन-चरण ग्रिड इंटीग्रेटेड एकाधिक सोलर पीवी सरणियाँ-बीईएस आधारित माइक्रोग्रिड में, मुख्य और सहायक वीएससी के डीसी लिंक को व्यक्तिगत अधिकतम पावर पॉइंट ट्रैकिंग (एमपीपीटी) तकनीक के माध्यम से अलग-अलग सोलर पीवी सरणियों के साथ एकीकृत किया जाता है। वीएससी टर्मिनल सामान्य युग्मन (पीसीसी) के बिंदु पर समानांतर में जुड़े हुए हैं, जो माइक्रोग्रिड की पावर रेटिंग को बढ़ाता है और उपयोगिता ग्रिड को सक्रिय बिजली वितरित करने के लिए माइक्रोग्रिड विस्तार की सुविधा प्रदान करता है। यह संचालन के एक स्वायत्त मोड में माइक्रोग्रिड की विश्वसनीयता में भी सुधार करता है। सामान्य परिचालन स्थिति के तहत, मुख्य वीएससी के लिए ग्रिड इंटरएक्टिव मोड में करंट नियंत्रण का उपयोग किया जाता है, जबकि ग्रिड की आउटेज पर, यह पीसीसी पर आवृत्ति और वोल्टेज को बनाए रखने के लिए वोल्टेज नियंत्रण के साथ संचालित होता है। सहायक वीएससी को एक गुणवत्ता वोल्टेज प्रदान किया जाता है, इसलिए इसके संचालन के लिए करंट नियंत्रण का उपयोग किया जाता है। ग्रिड इंटरएक्टिव मोड में, ग्रिड माइक्रोग्रिड पर वोल्टेज और आवृत्ति को बनाए रखता है। इसलिए, दोनों वीएससी करंट नियंत्रण एल्गोरिदम के साथ काम करते हैं।

माइक्रोग्रिड की पावर रेटिंग बढ़ाने के लिए, ग्रिड आउटेज परिदृश्य को हल करने और वितरण नेटवर्क के गुणवत्ता (पीक्यू) मुद्दों के समाधान के लिए, तीन चरण मल्टीपल सौर पीवी सरणियों के कई विन्यास-बीईएस आधारित माइक्रोग्रिड

को मुख्य वीएससी के डीसी लिंक पर बैटरी कनेक्शन यानी सीधे या द्विदिश कनवर्टर के माध्यम से, बिजली रूपांतरण चरणों जैसे , सिंगल स्टेज या डबल स्टेज और तीन-चरण सप्लाइ यानी तीन-चरण तीन-तार और तीन-चरण चार-तार सिस्टम के आधार पर वर्गीकृत किया जाता है । तीन-चरण ग्रिड एकीकृत एकाधिक सौर पीवी सरणियाँ -बीईएस आधारित माइक्रोग्रिड में, एक पीवी सरणी मुख्य वीएससी डीसी लिंक पर एक डबल चरण कॉन्फिगरेशन में एकीकृत होती है, जिसमें डीसी-डीसी बूस्ट कनवर्टर का उपयोग पहले चरण में एमपीपीटी वोल्टेज प्राप्त करने के लिए किया जाता है। इसके अलावा, दूसरे चरण में, मुख्य वीएससी को यूटिलिटी ग्रिड से जोड़ा जाता है। बीईएस भी सीधे मुख्य वीएससी डीसी लिंक पर एकीकृत है और लोड लेवलिंग का प्रबंधन करता है। हालाँकि, दूसरा पीवी सरणी एकल चरण कॉन्फिगरेशन में जुड़ा हुआ है। तीन-चरण ग्रिड इंटीग्रेटेड एकाधिक सोलर पीवी सरणियाँ-बीईएस के साथ द्विदिश कनवर्टर आधारित माइक्रोग्रिड में, पीवी सरणियाँ सीधे सिंगल स्टेज कॉन्फिगरेशन में वीएससी के डीसी लिंक से जुड़े होते हैं। बीईएस को मुख्य वीएससी डीसी लिंक पर एक द्विदिश कनवर्टर के माध्यम से एकीकृत किया गया है, जो अपने डीसी लिंक वोल्टेज को एमपीपीटी मूल्य पर बनाए रखता है और बीईएस के चार्जिंग / डिस्चार्जिंग करंट को नियंत्रित करता है। तीन-चरण ग्रिड में एकीकृत एकाधिक सोलर पीवी सरणियाँ-आधारित माइक्रोग्रिड, विभिन्न पावर रेटिंग के दो पीवी सरणी, सिंगल स्टेज टोपोलॉजी में वीएससी के डीसी लिंक से जुड़े होते हैं और मुख्य वीएससी ग्रिड को सक्रिय पावर प्रदान करता है। दोनों मोड में, वीएससी अपने संबंधित टर्मिनलों पर लोड मांगों को नियंत्रित करते हैं। पीवी पावर फीड-फॉरवर्ड घटक का उपयोग सिस्टम की गतिशीलता को बढ़ाने और ग्रिड को सक्रिय बिजली वितरित करने के लिए किया जाता है। इन विन्यासों में उपयोग की जाने वाली करंट नियंत्रण तकनीक ग्रिड पर या ग्रिड बनाने वाले कनवर्टर पर, पीक्यू मुद्दों जैसे कि हार्मोनिक्स करंट एक्सटेन्शूशन और पावर फैक्टर करेक्शन को सुधारती है।

सौर पीवी सरणी बिजली की उपलब्धता नहीं होने पर, वीएससी मोड वितरण स्थिर कम्पेसाटर (डीएसटीएटीसीओएम) मोड में बदल जाता है और ग्रिड लोड को बिजली की आपूर्ति करता है। तीन-चरण चार-तार एकाधिकपीवी सरणियाँ-बीईएस माइक्रोग्रिड का उपयोग न्यूट्रल करंट शमन के लिए और तीन-चरण तीन-तार सिस्टम के अन्य सभी कार्यों को करने के लिए किया जाता है। ये कॉन्फिगरेशन रूफटॉप आवासीय, औद्योगिक और वाणिज्यिक भवनों, इलेक्ट्रिक ट्रेक्शन, इलेक्ट्रिक वाहन, ग्रामीण / दूरस्थ क्षेत्रों और पानी पंपिंग को बिजली वितरित करने में सक्षम हैं। विभिन्न स्थिर अवस्था और गतिशील स्थितियों के लिए मैटलैब/सिमुलिक प्लेटफॉर्म में एकल सौर पीवी सरणी-बीईएस के एक द्विदिश कनवर्टर सिस्टम और एकाधिकसौर पीवी सरणियाँ-बीईएस आधारित माइक्रोग्रिड के साथ तीन-चरण ग्रिड एकीकृत प्रणालियों के सिमुलेटेड प्रदर्शनों को प्रयोगात्मक परिणामों के साथ प्रयोगशाला में प्रोटोटाइप और आरटी-एलएबी प्लेटफॉर्म में हार्डवेयर में लूप-टेस्ट बेंच के माध्यम से वास्तविक समय नियंत्रक ओपल-आरटी (ओपी4510), से मान्य किया गया है।

# TABLE OF CONTENTS

	<b>Page No.</b>
Certificate	i
Acknowledgements	ii
Abstract	v
Table of Contents	ix
List of Figures	xxi
List of Tables	xxx
List of Abbreviations	xxxii
List of Symbols	xxxii
<b>CHAPTER I      INTRODUCTION</b>	<b>1-12</b>
1.1    General	1
1.2    State of Art for Multiple Solar PV Arrays-BES Based Microgrid	3
1.3    Scope of Work	7
1.4    Outline of Chapters	9
<b>CHAPTER II      LITERATURE REVIEW</b>	<b>13-24</b>
2.1    General	13
2.2    Literature Review	13
2.2.1      Control Techniques for Grid Integrated Solar PV-BES Based Microgrid	14
2.2.2      Control Techniques for Standalone Solar PV-BES Based Microgrid	15
2.2.3      Control Techniques for Transient Free Transition Operation of Grid Integrated Solar PV-BES Based Microgrid	16
2.2.4      Control Techniques for Parallel Connected Power Converters in Solar PV-BES Based Microgrid	17
2.2.5      Control Techniques of Maximum Power Point Tracking for Solar Photovoltaic Battery Energy Storage Microgrid	17
2.2.6      Power Quality Issues and Mitigation Techniques of Solar PV-BES Based Microgrid	18
2.2.7      Control Techniques for Grid Integrated Solar PV System	19
2.3    Identified Research Areas	22
2.4    Conclusions	24
<b>CHAPTER III      CLASSIFICATION AND CONFIGURATIONS OF GRID INTEGRATED MULTIPLE SOLAR PV ARRAYS-BATTERY BASED MICROGRID SYSTEM</b>	<b>26-38</b>
3.1    General	26

3.2	Classification of grid integrated multiple solar PV arrays-BES based microgrid	26
3.3	Configurations of grid integrated multiple solar PV arrays-BES based microgrid	27
3.3.1	Configuration of Three-Phase Three-Wire Grid Integrated Solar PV-BES with Bidirectional Converter System	27
3.3.2	Configuration of Three-Phase Four-Wire Grid Integrated Solar PV-BES with Bidirectional Converter System	29
3.3.3	Configuration of Three-Phase Three-Wire Grid Integrated Multiple Solar PV Arrays-BES Based Microgrid	30
3.3.4	Configuration of Three-Phase Three-Wire Grid Integrated Multiple Solar PV Arrays-BES with Bidirectional Converter Based Microgrid	30
3.3.5	Configuration of Three-Phase Three-Wire Grid Integrated Multiple Solar PV Arrays-Based Microgrid	33
3.3.6	Configuration of Three-Phase Four-Wire Grid Integrated Multiple Solar PV Arrays-BES Based Microgrid	34
3.3.7	Configuration of Three-Phase Four-Wire Grid Integrated Multiple Solar PV Arrays-BES with Bidirectional Converter Based Microgrid	36
3.3.8	Configuration of Three-Phase Four-Wire Grid Integrated Multiple Solar PV Arrays- Based Microgrid	37
3.4	Conclusions	38
<b>CHAPTER IV</b>	<b>CONTROL AND OPERATION OF THREE-PHASE THREE-WIRE GRID INTEGRATED SOLAR PV-BES WITH BIDIRECTIONAL CONVERTER SYSTEM</b>	<b>40-75</b>
4.1.	General	40
4.2	System Configuration	40
4.3	Design of Three-Phase Three-Wire Grid Integrated Solar PV-BES with Bidirectional Converter System	41
4.4	Control Techniques for Three-Phase Three-Wire Grid Integrated Solar PV-BES with Bidirectional Converter System	43
4.4.1	MPPT Control Technique	43
4.4.2	Control for Voltage Source Converter	43
	4.4.2.1 Current Control Technique	44
	4.4.2.2 Voltage Control Technique	48
	4.4.2.3 Synchronization Controller	50
4.4.3	DC-DC Bidirectional Converter Controller	52
4.5	Results and Discussion	54
4.5.1	Simulated Performance of Three-Phase Three-Wire Grid Integrated Solar PV-BES with Bidirectional Converter System	54
	4.5.1.1 Simulated Steady State Performance under Grid Integrated Mode	55
	4.5.1.2 Simulated Steady State Performance under Off-Grid Mode	55

4.5.1.3	Simulated Dynamic Behaviour under Mode Transition from Grid Connected to Off-Grid Mode	56
4.5.1.4	Simulated Dynamic Behaviour under Mode Transition from Off-Grid Mode to Grid Connected Mode	57
4.5.1.5	Simulated Dynamic Behaviour under Load Unbalance	58
4.5.1.6	Simulated Dynamic Behaviour under Variation in Solar Insolation	58
4.5.1.7	Simulated Dynamic Behaviour under Variation in Load	60
4.5.1.8	Comparison of Ideal Discrete PR Controller with PI Controller	62
4.5.2	Experimental Performance of Three-Phase Three-Wire Grid Integrated Solar PV-BES with Bidirectional Converter System	65
4.5.2.1	Experimental Steady State Performance under Grid Integrated Mode	66
4.5.2.2	Experimental Steady State Behaviour under Off-Grid Mode	66
4.5.2.3	Experimental Dynamic Behaviour under Mode Transition from Grid Connected Mode to Off-Grid Mode	68
4.5.2.4	Experimental Dynamic Behaviour under Mode Transition from Off-Grid Mode to Grid Connected Mode	69
4.5.2.5	Experimental Dynamic Behaviour under Load Unbalance	69
4.5.2.6	Experimental Dynamic Behaviour under Variation in Solar Insolation	71
4.5.2.7	Experimental Dynamic Behaviour under Variation in Load	73
4.5.2.8	MPPT Performance at Two Insolation Levels	73
4.5.2.9	Experimental Dynamic Behaviour under Variation in Solar Insolation in Constant Power Mode	73
4.5.2.10	Experimental Dynamic Behaviour under Variation in Load in Constant Power Mode	74
4.6	Conclusions	75
<b>CHAPTER V</b>	<b>CONTROL AND OPERATION OF THREE-PHASE FOUR-WIRE GRID INTEGRATED SOLAR PV-BES WITH BIDIRECTIONAL CONVERTER SYSTEM</b>	<b>77-106</b>
5.1.	General	77
5.2	System Configuration	77
5.3	Design of Three-Phase Four-Wire Grid Integrated Solar PV-BES with Bidirectional Converter System	79

5.4	Control Techniques for Three-Phase Four-Wire Grid Integrated Solar PV-BES with Bidirectional Converter System	79
5.4.1	MPPT Control Technique	79
5.4.2	Control for Voltage Source Converters	79
5.4.2.1	Current Control Technique	79
5.4.2.2	Voltage Control Technique	83
5.4.2.3	Synchronization Controller	85
5.4.3	DC-DC Bidirectional Converter Controller	85
5.5	Results and Discussion	86
5.5.1	Simulated Performance of Three-Phase Four-Wire Grid Integrated Solar PV-BES with Bidirectional Converter System	86
5.5.1.1	Simulated Steady State Performance under Grid Integrated Mode	86
5.5.1.2	Simulated Steady State Performance under Off-Grid Mode	86
5.5.1.3	Simulated Dynamic Behaviour under Mode Transition from Grid Connected to Off-Grid Mode	86
5.5.1.4	Simulated Dynamic under Mode Transition from Off-Grid Mode to Grid Connected Mode	88
5.5.1.5	Simulated Dynamic Behaviour under Load Unbalance	92
5.5.1.6	Simulated Dynamic Behaviour under Variation in Solar Insolation	92
5.5.1.7	Simulated Dynamic Behaviour under Variation in Load	92
5.5.1.8	Comparison of Proposed Controller with PI Controller	94
5.5.2	Experimental Performance of Three-Phase Four-Wire Grid Integrated Solar PV-BES with Bidirectional Converter System	98
5.5.2.1	Experimental Steady State Performance under Grid Integrated Mode	99
5.5.2.2	Experimental Steady State Performance under Off-Grid Mode	100
5.5.2.3	Experimental Dynamic Behaviour under Mode Transition from Grid Connected Mode to Off-Grid Mode	101
5.5.2.4	Experimental Dynamic Behaviour under Mode Transition from Off-Grid Mode to Grid Connected Mode	102
5.5.2.5	Experimental Dynamic Behaviour under Load Unbalance	102
5.5.2.6	Experimental Dynamic Behaviour under Variation in Solar Insolation	103
5.5.2.7	Experimental Dynamic Behaviour under Variation in Load	105
5.5.2.8	MPPT Performance at Two Insolation Levels	106

5.6	Conclusions	106
<b>CHAPTER VI</b>	<b>CONTROL AND OPERATION OF THREE-PHASE GRID INTEGRATED MULTIPLE SOLAR PV ARRAYS-BES BASED MICROGRID</b>	<b>108-144</b>
6.1	General	108
6.2	System Configuration	108
6.3	Design of Three-Phase Grid Integrated Multiple Solar PV Arrays-BES Based Microgrid	109
6.4	Control Techniques for Three-Phase Grid Integrated Multiple Solar PV Arrays-BES Based Microgrid	109
6.4.1	MPPT Control Technique	109
6.4.2	Control for Voltage Source Converters	111
6.4.2.1	Current Control Technique and Voltage Control Technique for Main VSC	112
6.4.2.2	Current Control Technique for Ancillary VSC	116
6.4.2.3	Synchronization Controller	117
6.5	Results and Discussion	118
6.5.1	Simulated Performance of Three-Phase Grid Integrated Multiple Solar PV Arrays-BES Based Microgrid	118
6.5.1.1	Simulated Behaviour of Harmonic Analysis under Grid Integrated and Off-Grid Modes	118
6.5.1.2	Simulated Behaviour under Mode Transition from Grid Connected to Standalone Mode	119
6.5.1.3	Simulated Behaviour under Mode Transition from Standalone Mode to Grid Connected Mode	121
6.5.1.4	Simulated Behaviour under Load Unbalance	122
6.5.1.5	Simulated Behaviour of under Variation in Solar Insolation	123
6.5.1.6	Simulated Behaviour under Variation in Load in Grid Integrated Mode	125
6.5.1.7	Simulated Behaviour under No Solar Power Generation and Variation in Load in Off Grid Mode	126
6.5.1.8	Comparison of Proposed Controller (hysteresis with PR Controller) with PI Controller	127
6.5.2	Performance of Three-Phase Grid Integrated Multiple Solar PV Arrays-BES Based Microgrid with Hardware in Loop Implementation	129
6.5.2.1	Harmonic Analysis of microgrid in Grid Integrated and Off-Grid Modes	130
6.5.2.2	Behaviour of Microgrid under Mode Transition from Grid Connected Mode to Off-Grid Mode	131
6.5.2.3	Behaviour of Microgrid under Mode Transition from Off-Grid Mode to Grid Connected Mode	132
6.5.2.4	Behaviour of Microgrid under Load Unbalance	133

	6.5.2.5	Behaviour of Microgrid under Variation in Solar Insolation	134
	6.5.2.6	Behaviour of Microgrid under Variation in Load in Grid Integrated Mode	139
	6.5.2.7	Behaviour of Microgrid under No Solar Power Generation and Variation in Load in Off Grid Mode	142
6.6	Conclusions		144
<b>CHAPTER VII CONTROL AND OPERATION OF THREE-PHASE GRID INTEGRATED MULTIPLE SOLAR PV ARRAYS-BES WITH BIDIRECTIONAL CONVERTER BASED MICROGRID</b>			<b>146-190</b>
7.1	General		146
7.2	System Configuration		147
7.3	Design of Three-Phase Grid Integrated Multiple Solar PV Arrays-BES with Bidirectional Converter Based Microgrid		148
7.4	Control Techniques for Three-Phase Grid Integrated Multiple Solar PV Arrays-BES with Bidirectional Converter Based Microgrid		148
	7.4.1	MPPT Control Technique	148
	7.4.2	Control for Voltage Source Converters	148
		7.4.2.1 Current Control Technique and Voltage Control Technique for Main VSC	150
		7.4.2.2 Current Control Technique for Ancillary VSC	153
		7.4.2.3 Synchronization Controller	155
	7.4.3	DC-DC Bidirectional Converter Controller Control	160
7.5	Results and Discussion		160
	7.5.1	Simulated Performance of Three-Phase Grid Integrated Multiple Solar PV Arrays-BES with Bidirectional Converter Based Microgrid	161
		7.5.1.1 Simulated Behaviour of Harmonic Analysis under Grid Integrated and Off-Grid Modes	161
		7.5.1.2 Simulated Behaviour under Mode Transition from Grid Connected to Off-Grid Mode	162
		7.5.1.3 Simulated Behaviour under Mode Transition from Off-Grid Mode to Grid Connected Mode	162
		7.5.1.4 Simulated Behaviour under Load Unbalance	164
		7.5.1.5 Simulated Behaviour under Variation in Solar Insolation	165
		7.5.1.6 Simulated Behaviour under Variation in Load in Grid Integrated Mode	167
		7.5.1.7 Simulated Behaviour under No Solar Power Generation and Variation in Load in Off Grid Mode	168
		7.5.1.8 Simulated Performance of Synchronization Controller	169
		7.5.1.9 Simulated Performance of DSOGI-FLL Controller	170

	7.5.1.10	Simulated Performance for Comparison of Proposed Controller (Hysteresis with Non-Ideal PR Controller) with PI Controller	173
7.5.2		Performance of Three-Phase Grid Integrated Multiple Solar PV Arrays-BES with Bidirectional Converter Based Microgrid with Hardware in Loop Implementation	175
	7.5.2.1	Harmonic Analysis of Microgrid under Grid Integrated and Off-Grid Modes	176
	7.5.2.2	Behaviour of Microgrid under Mode Transition from Grid Connected Mode to Off-Grid Mode	176
	7.5.2.3	Behaviour of Microgrid under Mode Transition from Off-Grid Mode to Grid Connected Mode	178
	7.5.2.4	Behaviour of Microgrid under Load Unbalance	179
	7.5.2.5	Behaviour of Microgrid under Variation in Solar Insolation	181
	7.5.2.6	Behaviour of Microgrid under Variation in Load in Grid Integrated Mode	185
	7.5.2.7	Behaviour of Microgrid under No Solar Power Generation and Variation in Load in Off Grid Mode	187
7.6		Conclusions	190

## **CHAPTER VIII CONTROL AND OPERATION OF THREE-PHASE GRID INTEGRATED MULTIPLE SOLAR PV ARRAYS-BASED MICROGRID 191-227**

8.1		General	191
8.2		System Configuration	192
8.3		Design of Three-Phase Grid Integrated Multiple Solar PV Arrays-Based Microgrid	193
8.4		Control Techniques for Three-Phase Grid Integrated Multiple Solar PV Arrays- Based Microgrid	193
	8.4.1	MPPT Control Technique	193
	8.4.2	Control for Voltage Source Converters	193
		8.4.2.1 Current Control Technique and Voltage Control Technique for Main VSC	193
		8.4.2.2 Current Control Technique for ancillary VSC	198
		8.4.2.3 Synchronization Controller	199
8.5		Results and Discussion	200
	8.5.1	Simulated Performance of Three-Phase Grid Integrated Multiple Solar PV Arrays- Based Microgrid	200
		8.5.1.1 Simulated Behaviour of Harmonic Analysis under Grid Integrated and Off-Grid Modes	200
		8.5.1.2 Simulated Behaviour under Mode Transition from Grid Connected to Off-Grid Mode	201
		8.5.1.3 Simulated Behaviour under Mode Transition from Standalone Mode to Grid Connected Mode	203
		8.5.1.4 Simulated Behaviour under Load Unbalance	204

8.5.1.5	Simulated Behaviour under Variation in Solar Insolation	205
8.5.1.6	Simulated Behaviour under Variation in Load in Grid Integrated Mode	207
8.5.1.7	Simulated Behaviour under Variation in Load in Off-Grid Mode	208
8.5.1.8	Simulated Performance of Synchronization Controller	209
8.5.1.9	Simulated Performance of DSOGI-FLL Controller	210
8.5.1.10	Simulated Performance for Comparison of Proposed Controller (Hysteresis with Non-Ideal PR Controller) with PI Controller	210
8.5.2	Performance of Three-Phase Grid Integrated Multiple Solar PV Arrays-Based Microgrid with Hardware in Loop Implementation	212
8.5.2.1	Harmonic Analysis of Microgrid under Grid Integrated and Off-Grid Modes	213
8.5.2.2	Behaviour of Microgrid under Mode Transition from Grid Connected Mode to Off-Grid Mode	213
8.5.2.3	Behaviour of Microgrid under Mode Transition from Off-Grid Mode to Grid Connected Mode	215
8.5.2.4	Behaviour of Microgrid under Load Unbalance	215
8.5.2.5	Behaviour of Microgrid under Variation in Solar Insolation	219
8.5.2.6	Behaviour of Microgrid under Variation in Load in Grid Integrated Mode	223
8.5.2.7	Behaviour of Microgrid under Variation in Load in Off-Grid Mode	225
8.6	Conclusions	227
<b>CHAPTER IX CONTROL AND OPERATION OF THREE-PHASE FOUR-WIRE GRID INTEGRATED MULTIPLE SOLAR PV ARRAYS- BES BASED MICROGRID</b>		<b>228-269</b>
9.1	General	228
9.2	System Configuration	229
9.3	Design of Three-Phase Four-Wire Grid Integrated Multiple Solar PV Arrays-BES Based Microgrid	230
9.4	Control Techniques for Three-Phase Four-Wire Grid Integrated Multiple Solar PV Arrays-BES Based Microgrid	230
9.4.1	MPPT Control Technique	230
9.4.2	Control for Voltage Source Converters	232
9.4.2.1	Current Control Technique and Voltage Control Technique for Main VSC	232
9.4.2.2	Current Control Technique for ancillary VSC	235
9.4.2.3	Synchronization Controller	237
9.5	Results and Discussion	240

9.5.1	Simulated Performance of Three-Phase Four-Wire Grid Integrated Multiple Solar PV Arrays-BES Based Microgrid	240
9.5.1.1	Simulated Behaviour of Harmonic Analysis under Grid Integrated and Off-Grid Modes	240
9.5.1.2	Simulated Behaviour under Mode Transition from Grid Connected to Off-Grid Mode	241
9.5.1.3	Simulated Behaviour under Mode Transition from Off-Grid Mode to Grid Connected Mode	243
9.5.1.4	Simulated Behaviour under Load Unbalance	244
9.5.1.5	Simulated Behaviour under Variation in Solar Insolation	244
9.5.1.6	Simulated Behaviour under Variation in Load in Grid Integrated Mode	247
9.5.1.7	Simulated Behaviour under No Solar Power Generation and Variation in Load in Off-Grid Mode	248
9.5.2	Performance of Three-Phase Four-Wire Grid Integrated Multiple Solar PV Arrays-BES Based Microgrid with Hardware in Loop Implementation	250
9.5.2.1	Harmonic Analysis of Microgrid under Grid Integrated and Off-Grid Modes	250
9.5.2.2	Behaviour of Microgrid under Mode Transition from Grid Connected Mode to Off-Grid Mode	250
9.5.2.3	Behaviour of Microgrid under Mode Transition from Off-Grid Mode to Grid Connected Mode	252
9.5.2.4	Behaviour of Microgrid under Load Unbalance	255
9.5.2.5	Behaviour of Microgrid under Variation in Solar Insolation	258
9.5.2.6	Behaviour of Microgrid under Variation in Load in Grid Integrated Mode	263
9.5.2.7	Behaviour of Microgrid under No Solar Power Generation and Variation in Load in Off-Grid Mode	266
9.6	Conclusions	269
<b>CHAPTER X</b>	<b>CONTROL AND OPERATION OF THREE-PHASE FOUR-WIRE GRID INTEGRATED MULTIPLE SOLAR PV ARRAYS BES WITH BIDIRECTIONAL CONVERTER BASED MICROGRID</b>	<b>270-308</b>
10.1	General	270
10.2	System Configuration	271
10.3	Design of Three-Phase Four-Wire Grid Integrated Multiple Solar PV Arrays-BES with Bidirectional Converter Based Microgrid	272
10.4	Control Techniques for Three-Phase Four-Wire Grid Integrated Multiple Solar PV Arrays-BES with Bidirectional Converter Based Microgrid	272
10.4.1	MPPT Control Technique	272

10.4.2	Control for Voltage Source Converters	272
10.4.2.1	Current Control Technique and Voltage Control Technique for Main VSC	274
10.4.2.2	Current Control Technique for ancillary VSC	277
10.4.2.3	Synchronization Controller	279
10.4.3	DC-DC Bidirectional Converter Controller Control	280
10.5	Results and Discussion	280
10.5.1	Simulated Performance of Three-Phase Four-Wire Grid Integrated Multiple Solar PV Arrays-BES with Bidirectional Converter Based Microgrid	281
10.5.1.1	Simulated Behaviour of Harmonic Analysis in Grid Integrated and Off-Grid Modes	281
10.5.1.2	Simulated Behaviour under Mode Transition from Grid Connected to Off-Grid Mode	281
10.5.1.3	Simulated Behaviour under Mode Transition from Off-Grid Mode to Grid Connected Mode	283
10.5.1.4	Simulated Behaviour under Load Unbalance	285
10.5.1.5	Simulated Behaviour under Variation in Solar Insolation	286
10.5.1.6	Simulated Behaviour under Variation in Load in Grid Integrated Mode	288
10.5.1.7	Simulated Behaviour under Variation in Load and No Solar Power Generation in Off-Grid Mode	288
10.5.2	Performance of Three-Phase Four-Wire Grid Integrated Multiple Solar PV Arrays-BES with Bidirectional Converter Based Microgrid with Hardware in Loop Implementation	289
10.5.2.1	Harmonic Analysis of Microgrid in Grid Integrated and Off-Grid Modes	291
10.5.2.2	Behaviour of Microgrid under Mode Transition from Grid Connected Mode to Off-Grid Mode	291
10.5.2.3	Behaviour of Microgrid under Mode Transition from Off-Grid Mode to Grid Connected Mode	292
10.5.2.4	Behaviour of Microgrid under Load Unbalance	295
10.5.2.5	Behaviour of Microgrid under Variation in Solar Insolation	296
10.5.2.6	Behaviour of Microgrid under Variation in Load Load in Grid Integrated Mode	303
10.5.2.7	Behaviour of Microgrid under No Solar Power Generation and Variation in Load in Off Grid Mode	306
10.6	Conclusions	308

**CHAPTER XI CONTROL AND OPERATION OF THREE-PHASE FOUR-WIRE GRID INTEGRATED MULTIPLE SOLAR PV ARRAYS- BASED MICROGRID 310-346**

11.1	General	310
11.2	System Configuration	311

11.3	Three-Phase Four-Wire Grid Integrated Multiple Solar PV Arrays-Microgrid	312
11.4	Control Techniques for Three-Phase Four-Wire Grid Integrated Multiple Solar PV Arrays-without BES Based Microgrid	312
11.4.1	MPPT Control Technique	312
11.4.2	Control for Voltage Source Converters	312
11.4.2.1	Current Control Technique and Voltage Control Technique for Main VSC	313
11.4.2.2	Current Control Technique for ancillary VSC	317
11.4.2.3	Synchronization Controller	319
11.5	Results and Discussion	319
11.5.1	Simulated Performance of Three-Phase Four-Wire Grid Integrated Multiple Solar PV Arrays Based Microgrid	320
11.5.1.1	Simulated Behaviour of Harmonic Analysis in Grid Integrated and Off-Grid Modes	320
11.5.1.2	Simulated Behaviour under Mode Transition from Grid Connected to Off-Grid Mode	320
11.5.1.3	Simulated Behaviour under Mode Transition from Off-Grid Mode to Grid Connected Mode	321
11.5.1.4	Simulated Behaviour under Load Unbalance	323
11.5.1.5	Simulated Behaviour under Variation in Solar Insolation	325
11.5.1.6	Simulated Behaviour under Variation in Load in Grid Integrated Mode	327
11.5.1.7	Simulated Behaviour under Variation in Load in Off-Grid Mode	328
11.5.2	Performance of Three-Phase Four-Wire Grid Integrated Multiple Solar PV Arrays-Based Microgrid with Hardware in Loop Implementation	329
11.5.2.1	Harmonic Analysis of Microgrid under Grid Integrated and Off-Grid Modes	329
11.5.2.2	Behaviour of Microgrid under Mode Transition from Grid Connected Mode to Off-Grid Mode	329
11.5.2.3	Behaviour of Microgrid under Mode Transition from Off-Grid Mode to Grid Connected Mode	332
11.5.2.4	Behaviour under Load Unbalance	334
11.5.2.5	Behaviour of Microgrid under Variation in Solar Insolation	336
11.5.2.6	Behaviour of Microgrid under Variation in Load in Grid Integrated Mode	342
11.5.2.7	Behaviour of Microgrid under Variation in Load in Off-Grid Mode	345
11.6	Conclusions	346

**CHAPTER XII MAIN CONCLUSIONS AND SUGGESTIONS FOR FURTHER WORK 348-352**

12.1	General	348
12.2	Main Conclusions	349
12.3	Suggestions for Further Work	352
<b>REFERENCES</b>		<b>353-364</b>
<b>APPENDICES</b>		<b>365-385</b>
<b>LIST OF PUBLICATIONS</b>		<b>386-388</b>
<b>BIODATA</b>		<b>389</b>

## LIST OF FIGURES

Fig. 3.1	Classification of grid integrated multiple solar PV arrays-BES based microgrid system
Fig. 3.2	Configuration of three-phase three-wire grid integrated solar PV-BES with bidirectional converter system
Fig. 3.3	Configuration three-phase four-wire grid integrated solar PV-BES with bidirectional converter system
Fig. 3.4	Configuration of three-phase three-wire grid integrated multiple solar PV arrays-BES based microgrid
Fig. 3.5	Configuration of three-phase three-wire grid integrated multiple solar PV arrays-BES with bidirectional converter based microgrid
Fig. 3.6	Configuration of three-phase three-wire grid integrated multiple solar PV arrays-based microgrid
Fig. 3.7	Configuration of three-phase four-wire grid integrated multiple solar PV arrays-BES based microgrid
Fig. 3.8	Configuration of three-phase four-wire grid integrated multiple solar PV arrays-BES with bidirectional converter based microgrid
Fig. 3.9	Configuration of three-phase four-wire grid integrated multiple solar PV arrays-based microgrid
Fig. 4.1	System structure
Fig. 4.2	(a) Normalized gradient adaptive regularization factor based neural filter current control algorithm for VSC, (b) Block diagram of neural filter based control algorithm of phase ‘a’
Fig. 4.3	Voltage control technique for VSC
Fig. 4.4	Phase angle matching by PI controller
Fig. 4.5	Mode transition controller
Fig. 4.6	Synchronization control: (a) Phase angle generation in islanded mode of operation of main VSC, (b) SSS (G) signal generation for state ‘1’ or ‘0’ corresponding to grid interactive mode and standalone mode
Fig. 4.7	Bidirectional converter control
Fig. 4.8	Harmonic pattern of: (a) Load current, (b) Grid current
Fig. 4.9	Harmonic pattern of load voltage
Fig. 4.10	Response of system during grid connected to standalone mode
Fig. 4.11	Response of system during standalone mode to grid connected mode
Fig. 4.12	Internal signals of current control at load unbalance
Fig. 4.13	(a) System response at solar insolation change (b) System response at no solar power availability

Fig. 4.14	System response at load perturbation
Fig. 4.15	Harmonic pattern: (a) Load voltage with PR controller, (b) Load voltage with PI controller
Fig. 4.16	Comparison of ideal discrete PR controller with PI controller (a) $v_{La}$ , $v_{La}^*$ with ideal discrete PR controller (b) $v_{La}$ , $v_{La}^*$ with conventional PI controller (c) Bode plot of conventional PI controller with ideal discrete PR controller
Fig. 4.17	Experimental setup of developed prototype
Fig. 4.18	(a)-(j) Performance of current controller under steady state in grid integrated mode
Fig. 4.19	(a)-(g) Response of system under steady state in standalone mode
Fig. 4.20	(a)-(b) Response of internal signals of voltage control under steady state in standalone mode
Fig. 4.21	(a)-(b) Performance of system for the duration of grid connected to islanded mode
Fig. 4.22	(a)-(b) Performance of system for the duration of islanded to grid connected mode
Fig. 4.23	(a)-(c) Performance of system for internal signals of current controller under load removal of phase 'a' (d)-(f) Performance of system for internal signals of current controller under load injection of phase 'a' (g)-(h) Performance of system at Load removal of phase 'a' (i)-(j) Performance of system at Load injection of phase 'a'
Fig. 4.24	(a)-(d) Performance of system under grid tied mode for variation in solar irradiance
Fig. 4.25	(a)-(b) Behaviour of system for load change in grid interactive mode
Fig. 4.26	MPPT response of solar PV array at: (a) $600 \text{ W/m}^2$ , (b) $1000 \text{ W/m}^2$
Fig. 4.27	(a)-(b) Performance of system at constant power mode at solar variation
Fig. 4.28	(a)-(b) Performance of system under constant power mode under load variation
Fig. 5.1	System configuration
Fig. 5.2	VSC control
Fig.5.3	Principle of operation of hysteresis controller
Fig. 5.4	Harmonic pattern of: (a) Load current, (b) Grid current
Fig. 5.5	Harmonic pattern of load voltage
Fig. 5.6	(a)-(b) Performance of mode transition between off-grid to grid interactive modes
Fig. 5.7	(a)-(b) System performance during off-grid to grid intertied modes
Fig. 5.8	(a)-(b) System's response at load unbalance
Fig. 5.9	(a) Performance at no solar insolation (b) Behaviour at variation in solar insolation

Fig. 5.10	System response at load perturbation
Fig. 5.11	Harmonic pattern: (a) Load voltage with Park's transformation and inverse Park's based control and Mathews' algorithm based adaptive control (b) load voltage with PI controller
Fig. 5.12	Experimental setup of developed prototype
Fig. 5.13	(a)-(l) Response of system under steady state in grid interactive mode
Fig. 5.14	(a)-(g) System response under steady state in islanded mode
Fig. 5.15	(a)-(c) Performance of mode transition between utility grid interactive to off-grid modes:
Fig. 5.16	(a)-(c) Performance of mode transition between off-grid to grid interactive modes
Fig. 5.17	(a)-(e) System performance for load removal and insertion
Fig. 5.18	(a)-(b) System operation on non- accessibility of solar power (c)-(d) System response for solar insolation variation
Fig. 5.19	(a)-(b) System response in grid interactive mode at load variation
Fig. 5.20	MPPT behaviour: (a) at 600 W/m <sup>2</sup> , (b) at 1000 W/m <sup>2</sup>
Fig. 6.1	System configuration
Fig. 6.2	Control algorithm for Main VSC
Fig. 6.3	Control algorithm for ancillary VSC
Fig. 6.4	System harmonic spectra: (a) $i_{La1}$ , (b) $i_{sa}$
Fig. 6.5	System harmonic spectra: $v_{La}$
Fig. 6.6	(a)-(b) System's response for transition from grid interactive to off-grid mode
Fig. 6.7	(a)-(b) System's response transition from off-grid to grid connected mode
Fig. 6.8	(a)-(b) Response of system at load unbalance
Fig. 6.9	(a)-(b) Performance at no solar insolation
Fig. 6.10	(a)-(b) Behaviour at variation in solar insolation
Fig. 6.11	(a)-(b) Response at load change and grid intertied mode
Fig. 6.12	(a)-(b) Response of system in off-grid mode at no solar insolation and load variation
Fig. 6.13	Harmonic pattern: (a) Load voltage with discrete non-ideal PR controller, (b) Load voltage with PI controller
Fig. 6.14	Comparison of proposed controller (hysteresis with PR controller) with PI controller (a) $v_{La}$ , $v_{La}^*$ with ideal discrete PR controller (b) $v_{La}$ , $v_{La}^*$ with conventional PI controller (c) Bode plot of conventional PI controller with discrete non ideal PR controller

Fig. 6.15	OPAL-RT real time Test Bench
Fig. 6.16	Harmonic pattern of: (a) Load current, (b) Grid current
Fig. 6.17	Harmonic pattern of load voltage
Fig. 6.18	(a)-(d) Performance of system for transition from grid connected to islanded mode
Fig. 6.19	(a)-(d) Performance of system for the duration of islanded to grid connected mode
Fig. 6.20	(a)-(e) Response of system at load removal (f)-(j) Response of system at load insertion (k)-(l) Response of system at load removal and insertion
Fig. 6.21	(a)-(b) System performance at transition from maximum solar PV power to no PV power generation and vice/ versa (c)-(e) System performance at transition from maximum solar PV power to no PV power generation (f)-(h) Performance for variation from no solar PV power to peak solar power generation in grid connected mode
Fig. 6.22	(a)-(b) System behaviour at decrease in solar insolation in grid connected mode (c)-(d) Behaviour of system at increase in solar insolation in grid connected mode (e)-(f) Behaviour at fall and increase in solar insolation in grid connected mode
Fig. 6.23	(a)-(e) Response of system under load increase in grid connected mode (f)-(j) Response of system at load decrease in grid connected mode (k) Response of system under load increase and decrease in grid connected mode
Fig. 6.24	(a)-(e) System response in off-grid mode at no solar insolation and load increase (f)-(j) System response in off-grid mode at solar power available and load decrease
Fig. 7.1	System configuration
Fig. 7.2	Main VSC control
Fig. 7.3	Ancillary VSC control
Fig. 7.4	DSOGI-FLL: (a) Generation of positive sequence components, (b) Evaluation of in -phase and quadrature components, (c) FLL
Fig. 7.5	Mode transition controller
Fig. 7.6	Synchronization control: (a) Phase angle generation in islanded mode of operation of main VSC, (b) PES (S) signal generation for state '1' or '0' corresponding to grid connected mode and standalone mode
Fig. 7.7	System harmonic spectra: (a) $i_{La1}$ , (b) $i_{sa}$
Fig. 7.8	System harmonic spectrum of $v_{La}$
Fig. 7.9	(a)-(b) System performance during grid connected to off-grid mode
Fig. 7.10	(a)-(b) System performance for off-grid mode to grid connected mode
Fig. 7.11	(a)-(b) Response of system at load unbalance in grid connected mode
Fig. 7.12	(a)-(b) System performance at no solar insolation in grid connected mode

Fig. 7.13	(a)-(b) Behaviour at variation in solar insolation in grid connected mode
Fig. 7.14	(a)-(b) Response of system under load change in grid connected mode
Fig. 7.15	(a)-(b) System response in off-grid mode at no solar insolation and load variation
Fig. 7.16	Performance of synchronization controller
Fig. 7.17	Internal signals of DSOGI-FLL controller at grid reconnection
Fig. 7.18	Response of DSOGI-FLL during distortion in grid voltages
Fig. 7.19	Response of DSOGI-FLL control during unbalance in grid voltages
Fig. 7.20	Harmonic pattern: (a) load voltage with non-ideal PR controller, (b) load voltage with PI controller
Fig. 7.21	Comparison of proposed controller (hysteresis with non-ideal PR controller) with PI controller (a) $v_{La}$ , $v_{La}^*$ with non-ideal PR controller (b) $v_{La}$ , $v_{La}^*$ with conventional PI controller (c) Bode plot of conventional PI controller with non-ideal PR controller
Fig. 7.22	Harmonic pattern of: (a) Load current, (b) Grid current
Fig. 7.23	Harmonic pattern of: (a) load voltage with filter (b) load voltage without filter
Fig. 7.24	(a)-(d) Performance of system for the duration of grid connected to islanded mode
Fig. 7.25	(a)-(d) Performance of system for the duration of islanded to grid connected mode
Fig. 7.26	(a)-(f) Response of system at load removal (g)-(l) Response of system at load insertion
Fig. 7.27	(a)-(e) System performance at transition from peak solar PV power to no PV power generation (f)-(j) Performance for variation from no solar PV power to peak solar power generation in grid connected mode
Fig. 7.28	(a)-(d) System behaviour at decrease in solar insolation in grid connected mode: (e)-(h) Behaviour at increase in solar insolation in grid connected mode
Fig. 7.29	(a)-(e) Response of system under load increase in grid connected mode (f)-(j) Response of system at load decrease in grid connected mode
Fig. 7.30	(a)-(e) System response in off-grid mode at no solar insolation and load increase: (f)-(j) System response in off-grid mode at solar power available and load decrease
Fig. 8.1	System configuration
Fig. 8.2	Main VSC control
Fig. 8.3	Ancillary VSC control
Fig. 8.4	Microgrid system harmonic spectra (a) $i_{La1}$ , (b) $i_{sa}$
Fig. 8.5	Microgrid system harmonic spectrum of $v_{La}$

Fig. 8.6	(a)-(b) Microgrid performance during grid connected to off-grid mode
Fig. 8.7	(a)-(b) Microgrid performance during off-grid to grid connected mode
Fig. 8.8	(a)-(b) Response of system at load unbalance
Fig. 8.9	(a)-(b) Performance of system at no solar insolation
Fig. 8.10	(a)-(b) Behaviour of system at varying solar insolation
Fig. 8.11	(a)-(b) Response of system at load change
Fig. 8.12	System response in off-grid mode at variation in load
Fig. 8.13	Performance of synchronization controller
Fig. 8.14	Harmonic pattern: (a) Load voltage with non-ideal discrete PR controller, (b) Load voltage with PI controller
Fig. 8.15	Comparison of proposed controller (hysteresis with non-ideal PR controller) with PI controller (a) $v_{La}, v_{La}^*$ with non-ideal discrete PR controller (b) $v_{La}, v_{La}^*$ with conventional PI controller (c) Bode plot of conventional PI controller with non-ideal discrete PR controller
Fig. 8.16	Harmonic pattern of: (a) Load current, (b) Grid current
Fig. 8.17	Harmonic pattern of load voltage
Fig. 8.18	(a)-(e) Performance of system for the duration of grid connected to islanded mode
Fig. 8.19	(a)-(e) Performance of system for the duration of islanded to grid connected mode
Fig. 8.20	(a)-(f) Response of system at load removal (g)-(l) Response of system at load insertion
Fig. 8.21	(a)-(e) System performance at transition from peak solar PV power to no PV power generation (f)-(j) Performance for variation from no solar PV power to peak solar power generation in grid connected mode
Fig. 8.22	(a)-(e) System behaviour at decrease in solar insolation in grid connected mode (f)-(j) Behaviour at increase in solar insolation in grid connected mode
Fig. 8.23	(a)-(f) Response of system under load increase in grid connected mode (g)-(l) Response of system at load decrease in grid connected mode
Fig. 8.24	(a)-(f) System response in off-grid mode at no solar insolation and variation in load
Fig. 9.1	System structure
Fig. 9.2	Main VSC control
Fig. 9.3	Ancillary VSC control
Fig. 9.4	Synchronization control: (a) Phase angle generation in islanded mode of operation of main VSC, (b) PES ( $S$ ) signal generation for state '1' or '0' corresponding to grid connected mode and standalone mode

Fig. 9.5	Microgrid system harmonic spectra: (a) $i_{La1}$ , (b) $i_{sa}$
Fig. 9.6	Microgrid spectrum of $v_{La}$
Fig. 9.7	(a)-(b) Microgrid response for transition from grid integrated to off-grid mode
Fig. 9.8	(a)-(b) Microgrid's performance for transition from off-grid to grid connected mode
Fig. 9.9	(a)-(b) Response of system at load unbalance
Fig. 9.10	(a)-(b) Performance at no solar power
Fig. 9.11	(a)-(b) Response at solar insolation change
Fig. 9.12	(a)-(b) Response of system at load change
Fig. 9.13	(a)-(b) Performance of system in standalone mode during load change and under no solar power generation <sub>2</sub>
Fig. 9.14	Harmonic pattern of (a) Load current, (b) Grid current
Fig. 9.15	Harmonic pattern of load voltage
Fig. 9.16	(a)-(g) Performance of microgrid for the duration of grid interfaced to islanded mode
Fig. 9.17	(a)-(g) Performance of system for the duration of islanded to grid connected mode
Fig. 9.18	(a)-(h) Response of system at load removal (i)-(p) Response of system at load insertion
Fig. 9.19	(a)-(g) System performance at transition from peak solar PV power to no PV power generation (h)-(n) Performance for variation from no solar PV power to peak solar power generation in grid connected mode
Fig. 9.20	(a)-(g) System behaviour at decrease in solar insolation in grid connected mode: (h)-(n) Behaviour at increase in solar insolation in grid connected mode
Fig. 9.21	(a)-(h) Response of system under load increase in grid connected mode (i)-(p) Response of system at load decrease in grid connected mode
Fig. 9.22	(a)-(e) System response in off-grid mode at no solar insolation and load increase: (f)-(j) System response in off-grid mode at solar power available and load decrease
Fig. 10.1	System configuration
Fig. 10.2	Main VSC control
Fig. 10.3	Ancillary VSC control
Fig. 10.4	System harmonic spectra: (a) $i_{La1}$ , (b) $i_{sa}$ , (c) $v_{La}$
Fig. 10.5	System harmonic level of $v_{La}$
Fig. 10.6	(a)-(b) System performance during grid connected to off grid mode
Fig. 10.7	(a)-(b) System performance during off-grid mode to grid connected mode
Fig. 10.8	(a)-(b) Response of system at load unbalance

Fig. 10.9	(a)-(b) Performance of system at no solar insolation
Fig. 10.10	(a)-(b) System performance for change in solar insolation
Fig. 10.11	(a)-(b) Performance of system at load variation
Fig. 10.12	(a)-(b) System response in off-grid mode at load variation and no solar power insolation:
Fig. 10.13	Harmonic pattern of: (a) Load current, (b) Grid current
Fig. 10.14	Harmonic pattern of load voltage
Fig. 10.15	(a)-(g) Performance of system for the duration of grid interfaced to islanded mode
Fig. 10.16	(a)-(b) Performance of system for the duration of islanded to grid connected mode
Fig. 10.17	(a)-(g) Response of system at load removal (h)-(n) Response of system at load insertion
Fig. 10.18	(a)-(g) System performance at transition from peak solar PV power to no PV power generation (h)-(n) Performance for variation from no solar PV power to peak solar power generation in grid connected mode
Fig. 10.19	(a)-(g) System behaviour at decrease in solar insolation in grid connected mode: ( (h)-(n) Behaviour at increase in solar insolation in grid connected mode
Fig. 10.20	(a)-(g) Response of system under load increase in grid connected mode (h)-(n) Response of system at load decrease in grid connected mode
Fig. 10.21	(a)-(e) System response in off-grid mode at no solar insolation and load increase: (f)-(j) System response in off-grid mode at solar power available and load decrease
Fig. 11.1	System structure
Fig. 11.2	Main VSC control
Fig. 11.3	Ancillary VSC control
Fig. 11.4	Harmonic pattern of: (a) Load current, (b) Grid current
Fig. 11.5	Harmonic pattern of load voltage
Fig. 11.6	(a)-(b) Microgrid performance during grid connected mode to off-grid mode
Fig. 11.7	(a)-(b) Microgrid performance during off-grid to grid connected mode
Fig. 11.8	(a)-(b) Response of system at load unbalance
Fig. 11.9	(a)-(b) Performance at no solar power
Fig. 11.10	(a)-(b) Behaviour at solar insolation variation
Fig. 11.11	(a)-(b) Response of system at load change
Fig. 11.12	(a)-(b) System response in off-grid mode at variation in load
Fig. 11.13	Harmonic spectra of: (a) Load current, (b) Grid current

Fig. 11.14	Harmonic pattern of load voltage
Fig. 11.15	(a)-(g) Performance of system for the duration of grid connected to islanded mode
Fig. 11.16	(a)-(b) Performance of system for the duration of islanded to grid connected mode
Fig. 11.17	(a)-(f) Response of system at load removal (g)-(l) Response of system at load insertion (m) Response of system at load removal and load insertion
Fig. 11.18	(a)-(g) System performance at transition from peak solar PV power to no PV power generation (h)-(n) Performance for variation from no solar PV power to peak solar power generation in grid connected mode
Fig. 11.19	(a)-(g) System behaviour at decrease in solar insolation in grid connected mode: (h)-(n) Behaviour at increase in solar insolation in grid connected mode
Fig. 11.20	(a)-(f) Response of system under load increase in grid connected mode (g)-(l) Response of system at load decrease in grid connected mode (m) Response of system under load increase in grid connected mode
Fig. 11.21	(a)-(f) System response in off-grid mode under variation in load

## LIST OF TABLES

Table 4.1	Design parameters of three-phase three-wire grid integrated solar PV-BES with bidirectional converter system
Table 5.1	Design parameters of three-phase four-wire grid integrated solar PV-BES with bidirectional converter system
Table 6.1	Design parameters of three-phase grid integrated multiple solar PV arrays-BES based microgrid
Table 7.1	Design parameters of three-phase grid integrated multiple solar PV arrays-BES with bidirectional converter based microgrid
Table 8.1	Design parameters of three-phase grid integrated multiple solar PV arrays- based microgrid
Table 9.1	Design parameters of three-phase four-wire grid integrated multiple solar PV arrays-BES based microgrid
Table 10.1	Design parameters of three-phase four-wire grid integrated multiple solar PV arrays-BES with bidirectional converter based microgrid
Table 11.1	Design parameters of three-phase four-wire grid integrated multiple solar PV arrays-based microgrid

## LIST OF ABBREVIATIONS

RESs	Renewable energy sources
VSC	Voltage Source Converter
PV	Photo Voltaic
BES	Battery Energy storage
PCC	Point of Common Coupling
DC	Direct Current
AC	Alternating Current
PQ	Power Quality
MPPT	Maximum Power Point Tracking
SSS	Solid state switch
INC	Incremental Conductance
P&O	Perturb & Observe
PES	Power Electronics Switch
DSTATCOM	Distribution Static Compensator
ADC	Analog to Digital Converter
DAC	Digital to Analog Converter
DSO	Digital Storage Oscilloscope
PI	Proportional and Integral
PR	Proportional Resonant
MG	Microgrid
PLL	Phase Locked Loop
DSOGI-FLL	Dual Second-Order Generalized Integrator Frequency-Locked Loop
HIL	Hardware In Loop
THD	Total Harmonic Distortion
FFTPV	Feed-Forward Term of Solar Photovoltaic Power
IGBT	Insulated Gate Bipolar Transistor
QSG	Quadrature signals generator
SOGI-QSG ( $\alpha$ ) and SOGI-QSG ( $\beta$ )	Second-Order Generalized Integrator- Quadrature signals generator in $\alpha\beta$ reference frame

## LIST OF SYMBOLS

$v_{sab}, v_{sbc}$	Grid line voltages
$v_{sa}, v_{sb}, v_{sc}$	Sensed grid voltages for three phases
$V_t$	Amplitude of grid voltages
$u_{pa}, u_{pb}, u_{pc}$	In-phase unit templates
$i_{La}, i_{Lb}, i_{Lc}$	Load phase currents
$S_{pa}(q), S_{pb}(q), S_{pc}(q)$	Weight components for three phases
$\delta_{pa}(q)$	Output current error
$\psi_{pa}(q)$	Variable step size
$\rho_{pa}(q)$	Regularization factor
$\lambda, \sigma$	Initial step size parameter, small positive parameter
$H_{pa}(q)$	Cost function
$P_{pv}, P_{bt}$	PV power, battery power
$S_{pv}, S_{bt}$	Feed-forward terms due to $P_{pv}, P_{bt}$
$S_{pavg}$	Average weight of active load current
$S_{Lp}$	Amplitude of grid reference current
$i_{sa}, i_{sb}, i_{sc}$	Grid currents
$i_{sa}^*, i_{sb}^*, i_{sc}^*$	Grid reference currents
$i_{esa}, i_{esb}, i_{esc}$	Grid currents error
$V_r, \omega_{ref}$	Peak amplitude of load reference voltage, frequency
$v_{La}, v_{Lb}, v_{Lc}$	Sensed load voltages for three phases
$v_{La}^*, v_{Lb}^*, v_{Lc}^*$	Reference load phase voltages
$v_{Lar}, v_{Lbr}, v_{Lcr}$	Load phase voltages error
$i_{La}^*, i_{Lb}^*, i_{Lc}^*$	Reference load phase currents
$T_{La}(z), T_{Lb}(z), T_{Lc}(z)$	Transfer functions of PR controllers
$k_{dpv}, k_{div}$	Proportional and integral constants of discrete PR controller
$\theta_g, \theta_l$	Grid voltage angle, PCC voltage angle
$\Delta\theta, f_g$	Angle difference between Grid voltage and PCC voltage angle, Grid frequency
$V_{dc}$	Sensed DC link voltage
$V_{dc}^*$	Reference DC link voltage
$V_{dce}$	DC link voltage error
$C_{dc}$	DC link capacitance
$I_{bt}, I_{bt}^*$	Sensed and reference battery current
$I_{btr}$	Battery current error
$k_{pdc}, k_{idc}$ and $k_{pbt}, k_{ibt}$	Proportional and integral gains of DC link voltage and battery current control
$R_f, C_f$	Ripple filter resistance and capacitance
$L_f$	Interfacing Inductor
$L_b = L_{buck} = L_{boost}$	Buck -Boost converter inductance
$f_{sw}$	Switching frequency
$G_i$	Solar irradiance
$D_{buck}, D_{boost}$	Bidirectional converter: Duty cycles for buck mode, boost mode
$V_{oc}$	Open circuit voltage of PV array
$I_{sc}$	Short circuit current of PV array

$P_{mp}$	MPPT voltage
$I_{mp}$	MPPT current
$P_{pvmp}$	MPPT power
$m$	Modulation index
$h$	Overloading factor
$R_p, C_{pbat}$	Battery constituents
$i_{sn}, i_{Ln}, i_{vscn}$	Grid neutral current, load neutral current, VSC neutral current
$i_{sn}^*$	Reference neutral current
$L_{fn}$	Interfacing inductor neutral leg of VSC
$I_{pa}, I_{pb}, I_{pc}$	load active power constituents
$\tau, \psi_{pa}, \rho_{pa}, \eta_{pa}$	A small positive constant for convergence control, current error, gradient adaptive step size, estimate of a gradient vector
$I_{pLavg}$	Average of active power constituent
$I_{pnet}$	Grid reference current amplitude
$I_{pvw}$	PV weight component i.e. feed-forward part
$V_d, V_q$	Direct axis and quadrature axis components of load voltages from Park's transformation
$V_d^*, V_q^*$	Direct axis and quadrature axis reference voltages
$V_{erd}$	Error between direct axis and quadrature axis parts of load voltages and reference direct axis and quadrature parts axis
$I_d^*, I_q^*$	Direct axis and quadrature axis current components
$i_{Lfa}, i_{Lfb}, i_{Lfc}$	Load reference currents
$\omega_{comp}, \omega_{cop},$	Frequency constituents of synchronization controller
$\theta_{comp}, \theta_{cop}$	Angle obtained from frequency constituents of synchronization controller
$I_{bat}$	Battery current
$I_{bat}^*$	Battery reference current
$I_{bte}$	Battery current error
$I_{er}^*$	Current input to pulse width modulator of buck-boost converter
$D_{boost1}$	Duty cycle of boost converter
$V_{dc1}, V_{dc2}$	DC link Voltages for main and ancillary VSCs
$V_{dc1}^*, V_{dc2}^*$	Reference DC link Voltages for main and ancillary VSCs
$C_{dc1}, C_{dc2}$	DC link capacitor for main and ancillary VSCs
$N_{ss1}$ and $N_{pp1},$	Series and parallel modules for main VSC
$N_{ss2}$ and $N_{pp2}$	Series and parallel modules for ancillary VSC
$R_{ss}$ and $R_{pp}$	Series and parallel resistances for PV array
$P_{pv1}, P_{pv2}$	Solar PV array powers for main and ancillary VSCs
$V_{pv1}, V_{pv2}$	PV voltages main and ancillary VSCs
$I_{pv1}, I_{pv2}$	PV currents main and ancillary VSCs
$I_{pa1}, I_{pb1}, I_{pc1}$	Active power components of load currents for main VSCs
$I_{pa2}, I_{pb2}, I_{pc2}$	Active power components of load currents for ancillary VSCs
$\psi_{pa1}, \gamma_{pa1}, \eta, \zeta_{pa1}, \delta$	Current error, adaptable step size, scale factor, cross correlation between current error and input, forgetting factor
$I_{pLavg1}$ and $I_{pLavg2}$	Active power constituents for main and ancillary VSCs
$V_{dce1}$ and $V_{dce2}$	DC link voltage error for the main VSC and ancillary VSCs
$I_{l1}$ and $I_{l2}$	DC loss constituent for the main VSC and ancillary VSCs

$I_{wvpv1}$ and $I_{wvpv2}$	Feed-forward component for current control of main and ancillary VSCs
$I_{pnet1}$ and $I_{pnet2}$	Amplitude of grid reference current of main and ancillary VSCs
$V_p$ and $\omega_r$	Reference peak voltage amplitude and frequency for load voltages in multiple array microgrids
$T_a(z), T_b(z), T_c(z),$ $k_{pv}$ and $k_{iv}, \omega_{cu}$	Transfer functions of discrete non-ideal PR controller Proportional and integral gains, bandwidth around resonant frequency for discrete non-ideal PR controller
$i_{faload}, i_{fbload}, i_{fcload}$	Load reference currents
$i_{eLa}, i_{eLb}, i_{eLc}$	Load current errors
$V_{l1}$	PCC voltage amplitude
$u_{pa1}, u_{pb1}, u_{pc1}$	PCC voltages unit templates
$i_{sa1}, i_{sb1}, i_{sc1}$	Main VSC sensed grid currents
$i_{sa1}^*, i_{sb1}^*, i_{sc1}^*$	Main VSC reference grid currents
$i_{sa2}, i_{sb2}, i_{sc2}$	Ancillary VSC sensed grid currents
$i_{sa2}^*, i_{sb2}^*, i_{sc2}^*$ ,	Ancillary VSC reference grid currents
$i_{La1}, i_{Lb1}, i_{Lc1}$	Main VSC load currents
$i_{La2}, i_{Lb2}, i_{Lc2}$	Ancillary VSC load currents
$i_{vsca1}, i_{vsch1}, i_{vscc1}$	Main VSC's currents
$i_{vsca2}, i_{vsch2}, i_{vscc2}$	Ancillary VSC's currents
$i_s$	Grid currents
$i_{s1}, i_{L1}, i_{vsc1}$	Grid currents, load currents and VSC currents for main VSC
$i_{s2}, i_{L2}, i_{vsc2}$	Grid currents, load currents and VSC currents for ancillary VSC
$G_1, G_2$	Solar insolation intensity for PV array of main and ancillary VSCs
$\eta_1, \mu, \zeta_{pa1}, \beta_{pa1}$	Small positive constant for convergence control, gain, current error, gradient adaptive step size, gradient vector.
$T_a(s), T_b(s), T_{Lc}(s), \omega_{cf}$	Non-ideal PR controller's transfer functions, cut off frequency
$i_{fa}, i_{fb}, i_{fc}$	Load reference currents
$I_l$	DC loss component for the ancillary VSC
$I_{ebat}$	Battery current error
$k_{pbat}, k_{ibat}$	Proportional and integral gains of battery current control,
$\eta_{pa1}, \lambda, \delta_{pa1}, \psi_{pa1} \sigma$	Adjustable step size, convergence control parameter, current error, updating of step size by reducing the noise sequence, gain
$\phi_{pa1}, \varepsilon_{pa1}$	Adaptive step size, current error
$\lambda_{pa1}, \phi_{pa1}$	Gradient vector, current error in Benveniste algorithm
$\rho, \beta, \zeta_{pa1}$	Tuning parameter, parameter for convergence rate and adaptive step size of the control algorithm by Zou et-al
$i_{sn1}, i_{Ln1}, i_{vsen1}$	Grid neutral current, load neutral current and VSC neutral current for main VSC
$i_{sn2}, i_{Ln2}, i_{vsen2}$	Grid neutral current, load neutral current and VSC neutral current for ancillary VSC
$v_{s\alpha}$ and $v_{s\beta}$	90°-shifted grid voltages in $\alpha\beta$ reference frame
$v_{s\alpha}', v_{s\alpha}''$ and $v_{s\beta}', v_{s\beta}''$	In-phase and quadrature components through SOGI-QSG ( $\alpha$ ) and SOGI-QSG ( $\beta$ )
$e_\alpha, e_\beta$	Error signals of SOGI-QSG ( $\alpha$ ) and SOGI-QSG ( $\beta$ )
$e_\alpha'$ and $e_\beta'$	Frequency error variables

$\tau$	FLL gain
$v_{\alpha}^+, v_{\beta}^+$	Positive sequence components of grid voltages
$e_{avg}$	Average frequency error variable
$\omega_g'$	Estimated frequency from DSOGI-FLL